S. Alzahran, M.S. Islam, S. C. Saha, "Heat transfer augmentation in retrofitted corrugated plate heat exchanger", International Journal of Heat and Mass Transfer, 161 (2020) pp. 120226.

Heat transfer augmentation in retrofitted corrugated plate heat exchanger

Salman Al zahrani[1,2], Mohammad S. Islam[1], Suvash C. Saha[1,*]

[1]School of Mechanical and Mechatronic Engineering, University of Technology Sydney, Ultimo NSW 2007, Australia
[2] Mechanical Engineering Department, Faculty of Engineering, Al baha University, Saudi Arabia

HIGHLIGHTS

- Newly modified corrugated plate heat exchanger (CPHE) is proposed.
- Thorough comparison among the modified CPHE and other PHEs is carried out.
- The resulted turbulence kinetic energy of the modified channel is the highest.
- Overall thermal performance of the modified CPHE is the best.
- The best performance of the modified CPHE takes place at Re=1600.

Abstract

Corrugated plate heat exchangers (CPHEs) have been extensively adopted especially for systems that require high thermal efficiencies such as aerospace and gas turbine power plants. According to several factors (i.e. required heat duty), CPHEs can be optimized to meet the application requirements. However, the number of the required thermal plates (N_p) could be very large (N_p>40) which in turn would cause several disadvantages (i.e. sever flow maldistribution). Therefore, the present study aims to introduce an innovative modification that can boost the thermal performance of the basic CPHE which in turn would reduce the number of required plates for the same heat duty. The thermal performance of the modified CPHE has been numerically investigated by using Computational Fluid dynamics (CFD) software. The numerical data have been validated with experimental measurement from the literature. The impact of the new modification has been studied on Nusselt number (Nu), fanning friction factor (*f*), Stanton number (St), Turbulence kinetic energy (TKE), flow maldistribution, j factor, and quality index factor (JF). The result has been compared with previously reported data of the basic corrugated and flat PHEs. At the same mass flow rate, Nu, *f*, and TKE of the modified CPHE are respectively 1.3, 1.7, and 3.5 times greater than those of the basic CPHE. Moreover, JF data of the modified CPHE are 1.4, and 64 times greater than those of the basic corrugated and flat PHEs, respectively. In addition to the superior thermal performance, the present modification offers larger contact area between the plates which could boost the overall mechanical integrity of the heat exchanger. Thus, this modification could pave the way for CPHEs to be incorporated in new applications that require more compact and durable HEs. The heat transfer correlations of the modified CPHE have been developed.

Keywords: Plate heat exchanger; Chevron angle; Heat transfer; Enhancement; Nusselt number; Single-phase.

1. Introduction

The continuous global demand on energy represents a driving force to develop new generation of the compact heat exchangers (CHEs). In the next two decades, the global demand on energy is expected to increase by 37% [1]. CPHE is the most common type of CHE, which was introduced at 1920's and it was mainly used for milk pasteurization. Firstly, CPHE was made from cast metal plates stacked inside a frame. The temperature and pressure limitations were the main disadvantages for PHE to be used in more aggressive applications i.e. acid coolers. However, the advancement in the material technology allows CPHE to be used for higher pressure and temperature applications [2]. Although the thermal performance of CPHE is extraordinary, but the air conditioning and refrigerant companies could not adopt this technology immediately because of the use of the gaskets for sealing [3]. However, welded PHE has been introduced to eliminate the gaskets' use. Nowadays, welded CPHEs are used for heating, ventilation, and air conditioning systems (HVAC) and ammonia cooling units [3]. In addition to the high thermal efficiency of CPHE, its weight and volume are respectively 20% and 30% compared to shell and tube heat exchanger for the same heat transfer area [4].

Nomenclature

A	Effective heat transfer area, m^2	Greek	
$A_\circ$	Croos-sectional channel flow heat transfer area, m^2	β	Chevron angle, °
A_P	Cross-sectional area of the inlet port, m^2	μ	Dynamic viscosity, $Pa.s$
C_p	Specific heat, $J/kg.k$	μ_t	Turbulent viscosity, $Pa.s$
d_e	Equivalent diameter	ρ	Fluid density, kg/m^3
f	Fanning friction factor	Subscripts	
j	Colburn factor, $j = \frac{Nu}{RePr^{1/3}}$	avg	Average
JF	JF factor	b	Bulk fluid temperature
h	Convective heat transfer coefficient, W/m^2K	c	Cold stream
L_h	Horizontal length from port to port, m	CPHE	Corrugated plate heat exchanger
L_p	plate's channel effective length, m	FPHE	Flat plate heat exchanger
L_v	vertical length from port to port, m	HE	Heat exchanger
L_w	flow channel width, m	h	Hot stream
N	Number of channels	i	Inlet condition
Nu	Nusselt number	m	Measured
Q	Heat transfer rate, W	o	Smooth (FPHE)
P_m	Overall pressure drop, Pa	w	Wall
P_{mal}	Flow maldistribution intensity	mal	Maldistribution
Re	Reynolds number	i, j, k	Coordinates
St	Stanton number, $St = \frac{Nu}{RePr}$		
S_k	User define source		
S_ε			
t	Plate thickness, m		

Also, for the same thermal performance, the volume of CPHE is 50% and 60% less than finned tube and serpentine HEs [5], respectively. Therefore, CPHE has widely spread out for chemical processing, pharmaceutical, polymers, industrial and many other applications.

Fluid flow visualization is highly important in order to reveal flow pattern, transition and turbulence onset points, stagnation areas etc. Fluid flow visualization inside CPHE has been

conducted by Fock and Knibbe [6]. A spiral flow was observed on the corrugations on each wall. Furthermore, the visual inspection inside corrugated channel that has been carried out by Tokgoz and Sahin [7] has reported that, the sharp corners are the main source for turbulence generation. Lozano et al. [8] have both experimentally and numerically investigated the fluid flow pattern for an oil-water inside the channels of CPHE. The planar laser-induced fluorescent (PLIF), and the particle image velocimetry (PIV) are employed to visualize the flow structure and the flow velocity respectively. The numerical and experimental results were consistent and they showed that, the flow is not uniform for both oil and water and it tends to flow along the lateral sides of the plates. The flow distribution and pressure drop inside two channels of CPHE were studied numerically by Tsai et al. [9]. The port effect was considered, and the fluid maldistribution formula that is proposed by Bssiouny and Martin [10] was adopted. However, the friction factor was used instead of the channel frictional coefficient (ζ_c) that is used in the genuine formula of Bssiouny and Martin [10]. An experimental study on the flow maldistribution was performed by Rao et al. [11]. The flow maldistribution found to be affected by the flow rate, the port size, and the number of channels. An important finding is that, the number of the plates should be carefully calculated, because at a certain point it will only cause a significant pressure drop rather than increasing the heat transfer area [11].

A comparison between different types of plate was carried out by Durmus et al. [12]. The chevron plate type is found to provide the highest heat transfer rate and pressure drop among the other types. Lin and Huang [13] have characterized the heat transfer performance of CPHE by deriving dimensionless correlations using Buckingham Pi theorem. The results show that, both mean and local Nu are greatly affected by Reynolds number (Re) and inclination angle "β". The basic features of the chevron plate are presented in Fig. 1. Fock et al. [14] investigated the effect of different $\beta's$ on heat transfer and pressure drop. The result showed that, β is the most important factor that strongly affect the heat transfer process. The reason is that, β changes the flow direction and consequently the performance of the CPHE. According to the same study, the maximum heat transfer rate occurred at $\beta = 80°$. Similar experimental studies have been carried out to further investigate the effect of chevron angle on the thermo-hydraulic performance of the CPHE [15, 16]. However, there is a significant variation between the results of the heat transfer correlations that have been provided by different researchers [14, 17]. As CPHE consists of consecutive plates, where each plate is rotated by 180° with respect to the adjacent plate, forming complicated 3-D criss-cross channel. Thus, each channel is made up from many geometrical parameters such as the corrugation depth, pitch, and roundness. Hence, different geometrical dimensions could contribute to the deviation between the previous studies [18].

Several techniques have been adopted by researchers in order to improve the thermal performance of the HEs. Gurel et al. [19] have applied the human lung pattern on the surfaces of the plates of the FPHE. They reported this design could enhance the heat transfer by about 71.3%. Modified design of the corrugated and the flat PHEs have been proposed by Zahrani et al.[20, 21]. The findings show the convective heat transfer has enhanced by ~75% and ~70% for corrugated and flat PHEs, respectively. Aliabadi et al. [22] have studied the quality of different passive techniques. They have found that, the winged wavy plates could provide the best thermal performance in comparison to other types of wavy plates i.e. perforated ones. In addition, several studies [23-26] have investigated the impact of adding various types of nanofluids (i.e. metal oxide nanofluids copper–water nanofluid, and carbon–water nanofluid) to the base fluid to improve the thermal performance of the CPHE. Generally, the findings

show similar trends where the heat transfer rate increases when they add nanofluids. However, the pressure drop is also increasing. Moreover, energy saving is an intrinsic aspect to be considered along with the operational and maintenance cost of the HE. Therefore, exergy loss analysis studies are necessary. Pandey and Nema [27] investigated the exergy loss of the CPHE with sinusoidal and rectangular corrugations' profiles. The results show lesser exergy loss and better contact between solid and fluid are achieved in case of sinusoidal profile. Similar findings have been found by Ipek et al. [28] when they investigated exergy loss for different corrugation's profile. Arsenyeva et al. [29] has developed a mathematical model to be used to optimize the shape of the corrugation. Furthermore, Lee et al. [30] has optimized the heat transfer area of the water side of the CPHE that was implemented in the low temperature heat pump system. An efficiency index for energy consumption of CPHE is proposed by Zhang et al. [31]. The formula of the efficiency index is proposed based on the single-phase heat transfer data of 281 CPHEs.

Several softwares have been developed to predict the behavior of the fluid flow and/or to resolve the boundary layers at the area of interest. CFD has been adopted to numerically predict different types of complicated phenomenon i.e. air flow over wing. Two approaches have been used to simulate fluid flow and heat transfer inside the CPHE: unitary cell and full-scale CPHE. A representative computational cell or a unitary cell is the smallest segment of the corrugated channel. To save a significant amount of the computational cost, several studies considered the periodicity of the heat transfer and the fluid flow pattern inside the channels of the CPHE by adopting the unitary cell approach [32, 33]. However, the validity of this approach is still questionable. Because there are various parameters that could affect the performance of CPHE, these parameters are not included in the unitary cell approach such as the port effect and the flow maldistribution on the plate's surface. Numerical study for the performance of the full-scale CPHE is carried out by Zahrani et al. [34]. Air and water as the process fluids have been investigated to explore the impact of Prandtl number (Pr) on the pressure drop and the heat transfer process.

Nowadays, the heat transfer enhancement is an essential target in order to reduce both the overall volume of the heat exchanger and the fuel consumption. The active technique requires an external input power such as surface vibration and jet impingement. On the other hand, the passive technique can be achieved either by using inserts such as twisted tape, or by performing a geometrical modification to the flow passage that could either enhance the flow mixing or reduce the pressure drop. Furthermore, the active technique is complicated in design, and hence the passive technique is the preferred one [35]. In PHEs, generally, the large number of thermal plates (N>40) would lead to two significant disadvantages [36]. These disadvantages are: severe flow maldistribution is more likely to take place, and the increase in overall heat transfer coefficient is negligible. In addition, the space for the HE to be installed will be larger and the cost of the HE will be higher. Therefore, the present study aims to present new passive technique that could simultaneously boost the thermo-hydraulic performance and the mechanical strength of the current well-known CPHE. Consequently, the number of the required thermal plates for the same heat duty would be less which in turn would save materials and mitigate the flow maldistribution. This modification has been applied on the surface of each thermal plate of the CPHE. Furthermore, the present modification could be implemented in any PHE without affecting the flow arrangements.

The effect of the present modification has been studied numerically. The results have been compared with the previously reported results of the basic corrugated [20] and flat [21] PHEs. For all three HEs, the geometrical dimensions, the physical properties, and the boundary conditions are identical. To attain a reliable result, the inlet/outlet ports, and the sinusoidal shape of the corrugations are considered in the numerical model. Each HE of the present PHEs comprises of four channels divided equally between the cold and the hot fluid. The numerical simulations have used single-phase water/water as the working fluids, U-type counter-current flow arrangement, $250 \leq Re \leq 2500$ and $\beta = 60°/60°$. Nusselt number, Stanton number, j factor, fanning friction factor, flow maldistribution intensity index, and JF factor are calculated to assess the thermal performance for each HE.

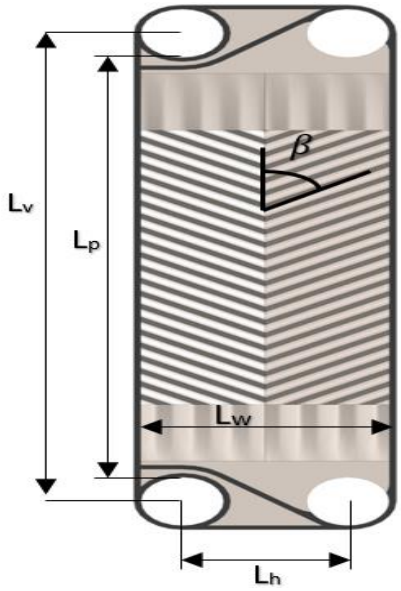

Fig. 1: Basic geometrical features of chevron plate.

2. Description of the new modification PHE.

CPHE is compact in nature, yet the present study suggests a new passive technique that would allow the CPHE to be even more compact. The flow in the well-known CPHE is either vertical or diagonal. However, the new CPHE can be employed for both vertical and diagonal flow. In addition, the flow arrangement used in this study is U-type counter-current flow. Yet, the new CPHE can also be employed in any flow arrangement e.g., Z-type, and parallel flow arrangement.

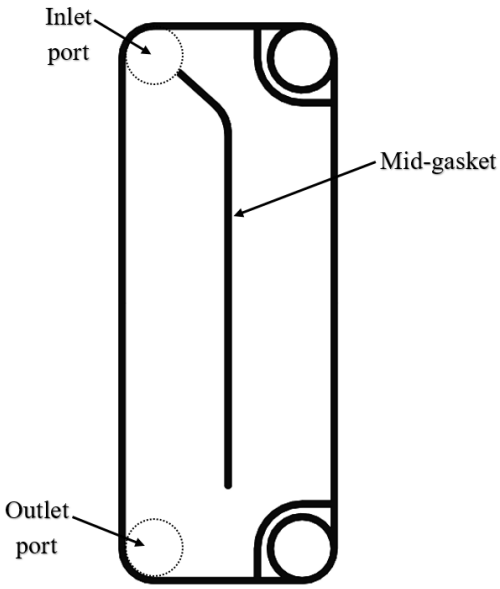

Fig. 2: The new gasket design.

Gasket is a mechanical seal, and mostly it is desirable to be made from materials that have the ability to deform and tightly seal the space between two or more mating surfaces. In the well-known CPHE, the gasket is compressed 25% of its original thickness to seal the space (the channel) between each two consecutive plates. Furthermore, the gasket regulates the fluid flow inside the channels of CPHE. In the new CPHE, the gasket is also used for the same objectives, but there is an additional gasket (mid-gasket) that starts from the corner of the inlet port from the middle side of the plate and ends right before the outlet port as shown in Fig. 2. As fluid enters from the inlet port, it gets separated between the two sides of the plate, then all fluids mix at the end of the middle gasket and exit from the outlet port. Simultaneously, on the adjacent plate, the other fluid follows the same flowing mechanism but in the opposite direction (counter-current) as shown in Fig. 3.

Fig. 3: Schematic of flow mechanism inside the modified CPHE.

3. Numerical approach

3.1 Governing equations and turbulence model

For numerical simulations, pressure-velocity coupling with SIMPLE algorithm have been adopted. For pressure, momentum, and energy, second order discretization is used. For turbulent kinetic energy, and turbulent dissipation rate, first order discretization is used. ANSYS FLUENT employs finite volume method (FVM). By this method, the partial differential equations (PDEs) are presented in the form of algebraic equations.

In order to calculate the changes in the physical and chemical properties of the fluid, ANSYS FLUENT solves all the governing equations. Navier Stokes equation (NS) (1) characterize the fluid's motion.

$$\frac{\partial}{\partial x_j}\left(\rho u_i u_j\right) = -\frac{\partial p}{\partial x_i} + \frac{\partial}{\partial x_j}\left[(\mu + \mu_t)\frac{\partial u_i}{\partial x_j}\right] \tag{1}$$

The left-hand side of NS represents the acceleration of the fluid, while the right-hand side represents the pressure and viscous forces that act on the fluid. Analytical solution may exist for special cases i.e. linear PDEs, or imposing simplified assumptions. Complicated flow problems have no analytical solution yet. However, CFD has the capabilities to numerically solve NS along with all other governing equations at each grid point in milliseconds until the solution gets converged.

For the fluid's flow, the mass of the fluid is always conserved regardless of the complexity of the channel or the flow direction. This fundamental principle is known as continuity of the flow. NS equations are always solved along with the continuity equation (2).

$$\frac{\partial}{\partial x_i}(\rho u_i) = 0 \tag{2}$$

In addition, FLUENT solves the energy equation (3) in order to resolve the heat transfer that occurs inside the heat exchanger.

$$\rho C_p \frac{\partial}{\partial x_j}\left(u_j T\right) = k_{eff}\frac{\partial^2 T}{\partial x_j^2} + (T_{ij})_{eff}\frac{\partial u_i}{\partial x_j} \tag{3}$$

All the numerical models (i.e. LES, DES, standard $k-\varepsilon$, and SST $k-\omega$) that are incorporated in Fluent solver have been tested in Zahrani et al. [20]. A realizable $k-\varepsilon$ with scalable wall function has been found the most accurate model. Thus, it is employed for the current investigation. More details about the turbulence model, and the transport equations, are provided in Zahrani et al. [20].

3.2 Model setup

The model has been generated by using Solidworks. The basic CPHE is the same one that was studied in Zahrani et al. [20]. The chevron angle is chosen as $60°/60°$ for both models. Furthermore, the geometrical dimensions are identical for both models. Each CPHE consists of four channels that are divided equally between the cold and the hot sides. The sinusoidal shapes have been created to construct the corrugations. Moreover, ports of the inlet and the outlet of both cold and hot sides will affect the flow distribution [37] inside the channels of the CPHE. Consequently, this would affect the pressure drop and the overall heat transfer process. Thus, the effect of the ports are considered in this study.

ANSYS meshing module is adopted for grids creation. A good mesh's metric qualities are difficult to be achieved for corrugated PHEs due to the existence of a large number of curved narrow passages. Thus, unstructured tetrahedral mesh elements are used as they are dedicated for complicated geometries where they can provide a good mesh quality easier than hexahedral elements [38]. The transition of tetrahedral elements from small mesh size in narrow passage and holes to larger size elsewhere is smoother and problem-free in comparison with hexahedral elements. However, hexahedral produces fewer elements and consequently faster solution. More efficient hexahedral mesh is achieved when the structured mesh is aligned to the physics [38]. Furthermore, to ensure the result is not affected by the grid's resolution, a grid sensitivity test has been performed as presented in Table 1 for the new corrugated PHE.

All simulations have been carried out for steady-state flow. The physical conditions are identical for both CPHEs. The plate's material is stainless steel. The cold and the hot sides have the same Reynolds number. Mass flow inlet is set at the inlet ports as the inlet boundary condition. The pressure at the outlet of the ports is set to be equal to the atmospheric pressure (zero gauge pressure) as the outlet boundary condition to prevent the occurrence of the reverse flow. An effective design of modern heat exchanger requires an efficient heat transfer in fluids and solids [39]. Usually fluids carry energy and solids are needed to allow the heat transfer to take place between the fluids without being mixed. Therefore, a conjugate heat transfer is set for both CPHEs with plate's thickness equal to 0.5 mm.

In the current investigation, the hot side is considered as the process fluid, therefore, all calculations are performed to the hot side.

Table 1: Mesh sensitivity test of the modified CPHE.

Grid's element (Million)	$T_{c,o}$	$T_{h,o}$	f
40	296.44	304.82	1.52
53	**296.44**	**304.61**	**1.46**
60.5	296.5	304.64	1.47

4. Results and discussion

4.1 Numerical approach validation

To validate the thermal performance of the present CPHEs, a non-dimensional standards parameters are adopted. Nu and *f* have been calculated and compared with other Nu and *f* data from the literature.

Although the differences in the geometrical parameters and physical conditions (e.g., corrugation's depth, wavelength, fluid viscosity, and density) could attribute in the deviation between the results, the present Nu data for the basic CPHE with $\beta = 60°/60°$ have been extensively validated in Zahrani et al. [20].

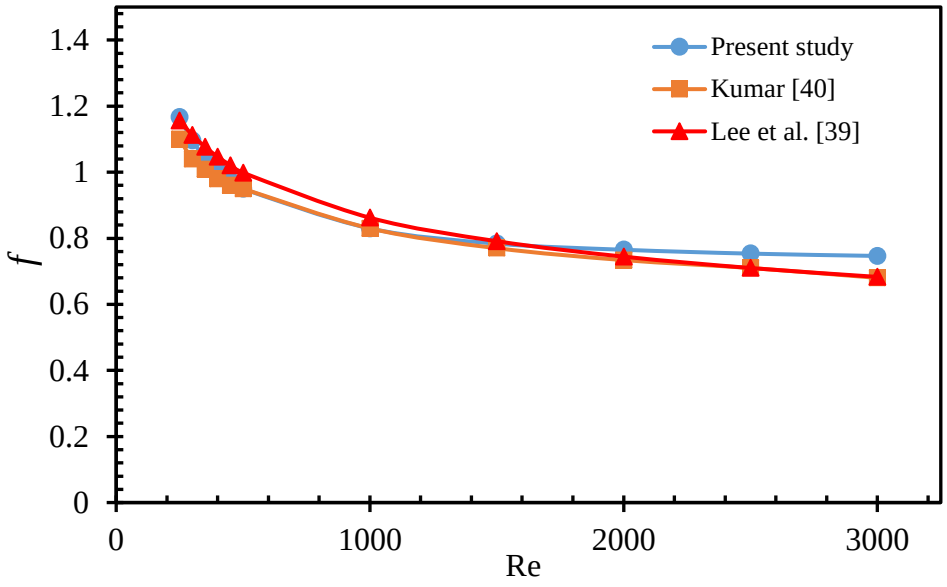

Fig. 4: Numerical versus experimental data of friction factor.

The numerical data of f for the basic CPHE with $\beta = 60°/60°$ are validated with the experimental correlation of Lee et al. [40], and Kumar [41]. The *f's* experimental correlation of Lee et al [40] is presented in Eq. 4 as follows:

$$f = 3.7235\, Re^{-0.2118} \tag{4}$$

Fig. 4 shows that, the present numerical *f* data are in good agreement with other *f* data from the literature. The enhancement of flow velocity results in the reduction of all the trends. The maximum deviation is +9.2%, and +9.3% with respect to the *f* data of Lee et al [40], and Kumar [41], respectively. The variation could be attributed to the difference in the geometrical dimensions (i.e. corrugation aspect ratio, and enlargement factor) where small difference could cause high variation in heat transfer and friction factor data [18].

4.2 Thermal performance evaluation

In the present study, a new modification to the design of the plates' surfaces is presented. The impact of this modification on the thermal performance of the CPHE has been numerically

investigated. The result has been compared with the previous studies of the basic corrugated and the flat PHEs [20, 21]. Fig. 5 illustrates the difference among the modified, basic, and smooth thermal plates. Hot and cold water are considered to be the working fluids.

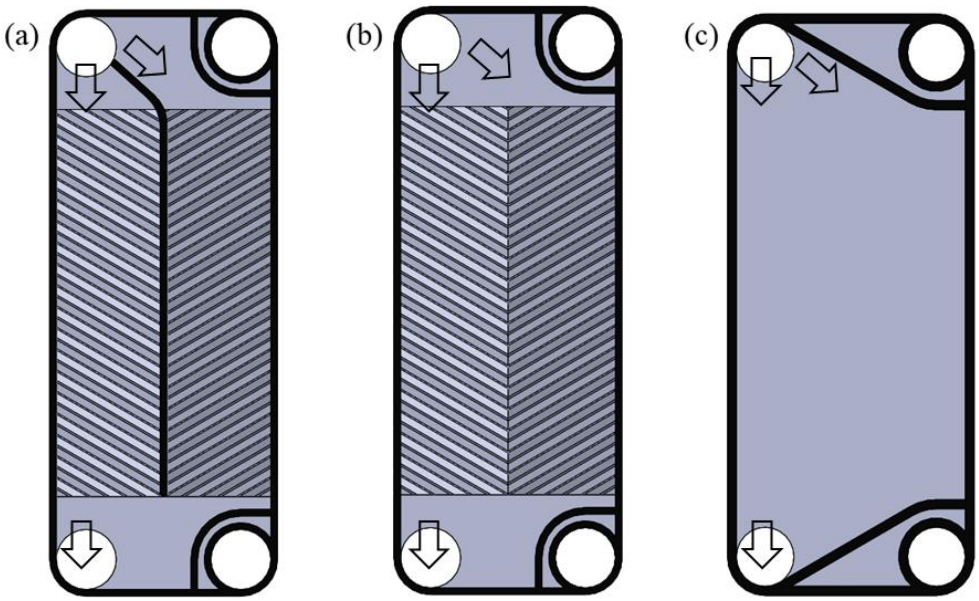

Fig. 5: Thermal plate of (a) modified CPHE, (b) basic CPHE, and (c) smooth FPHE.

All calculations are performed to the hot side as the process fluid. Although, the geometrical and physical conditions of all studies are identical, a dimensionless physical quantities are estimated in order to provide the most accurate data that are independent of the geometrical dimensions. Nu data with different Re are presented in Fig. 6. Nu data of the newly modified CPHE are found to be the highest. The enhancement in the convective heat transfer is up to 1.3 and 4 times greater than that of the basic corrugated and smooth PHEs, respectively.

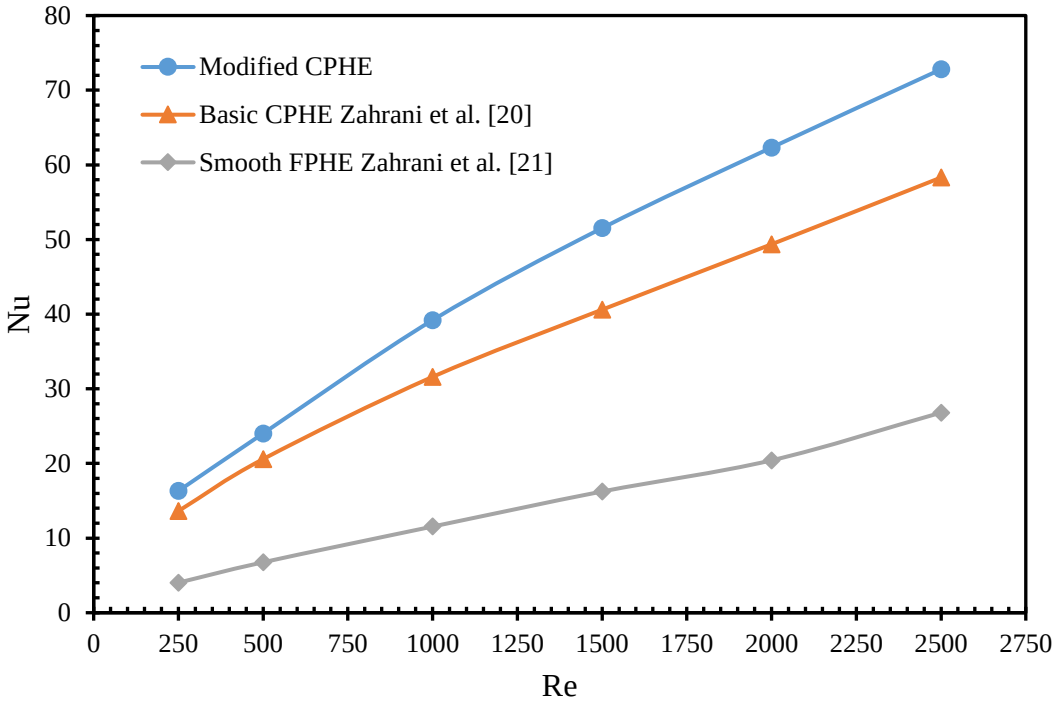

Fig. 6: Nu data versus Re for all investigated HEs.

In addition, in all cases Nu increases as Re increases because of the increase of mass flow rate ($\dot{m}$) where more $\dot{m}$ will lead to higher heat transfer coefficient (h). Furthermore, the thickness of the thermal boundary layers reduces as the mass flow rate increases, hence less thermal resistance is exerted by those boundary layers [34]. St is estimated and presented in Fig. 7. St of the modified HE yields the highest values with varying Re.

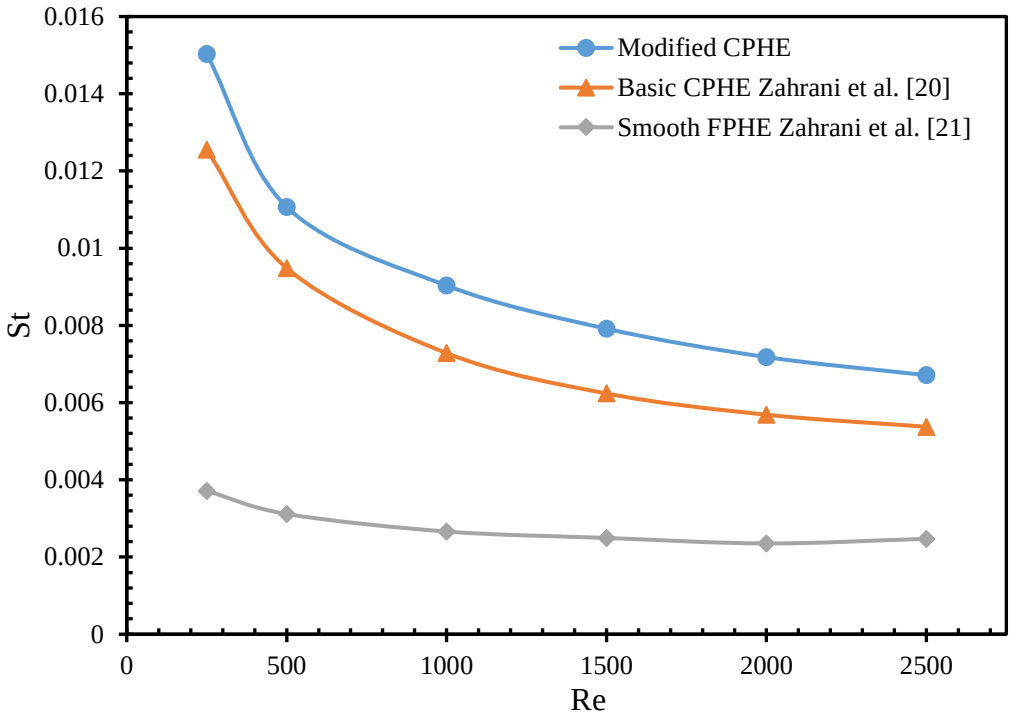

Fig. 7: St data versus Re for all investigated HEs.

From Nu and St figures, it is pronounced that the convective heat transfer rate inside the modified channels is higher than that of the basic channels. However, because the enhancement varies with Re, the enhancement percentage in the convective heat transfer due to the present new modification is estimated at different Re as:

$$Enhancement = \frac{(Nu - Nu_o)_{Modified} - (Nu - Nu_o)_{Basic}}{(Nu - Nu_o)_{Basic}} \times 100 \qquad (5)$$

Where Nu_o refers to Nusselt number of the FPHE (smooth channel). Fig. 8 shows the enhancement is fluctuating with Re. The minimum and the maximum enhancement in the convective heat transfer are taking place at Re~460 (16.7%) and Re~1600 (27%), respectively. In addition, at Re<460 and Re>1600 the enhancement's trend decreases. The reason could be that, the new modification boost the flow mixing at this range of Re i.e. 460<Re<1600, whereas the flow regimes in the modified and the basic channels at Re<460 and Re>1600 are similar i.e. laminar (Re<460), and turbulent (Re>1600). Furthermore, the entropy generation in this range (460<Re<1600) could be the lowest. However, the convective heat transfer rate inside the modified channel is greater than those of the basic one for all Re.

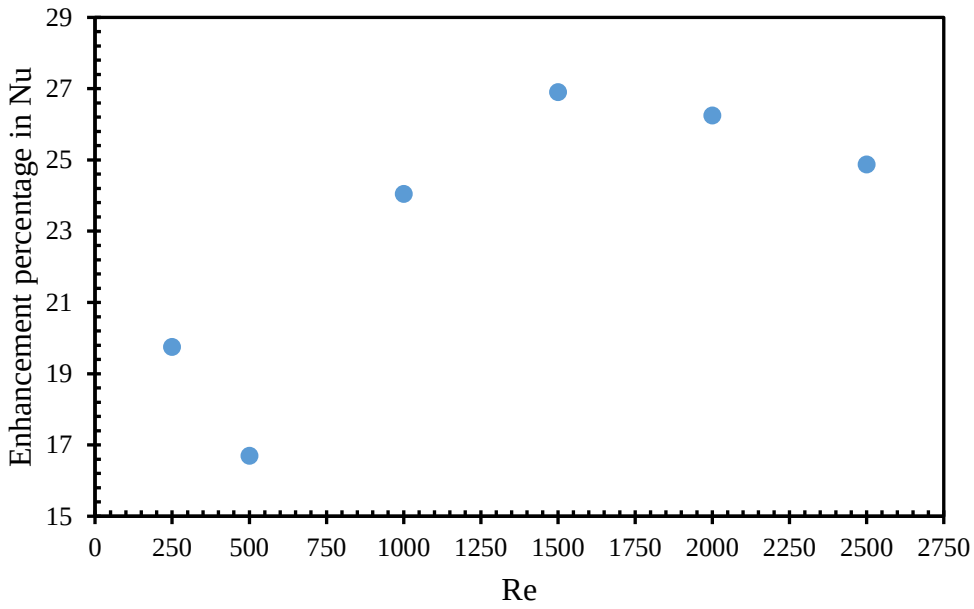

Fig. 8: The enhancement percentage of Nu versus Re.

The Colburn *j* factor is an index of thermal performance of the HEs and it is presented in Fig. 9 along with the fanning friction factor for each HE. The *j* and *f* data of the modified CPHE are greater than those of the basic CPHE and smooth PHE for all cases. The increase in the *f* data of the modified CPHE is up to 1.7 greater than that of the basic CPHE, and it is up to 25 times greater than that of the smooth PHE. Moreover, the *f* data of the basic CPHE are found 14 to 18 times higher than that of the smooth PHE.

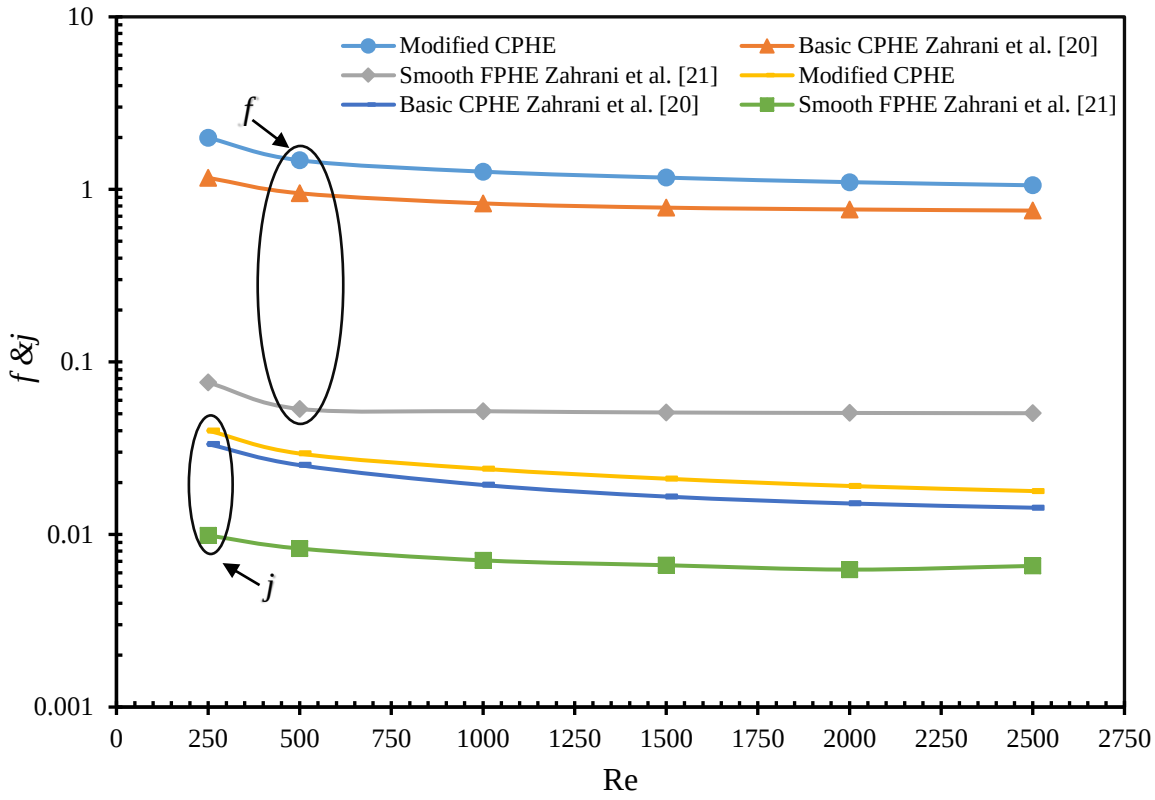

Fig. 9: Coulborn j and *f* data versus Re for all investigated HEs.

Furthermore, JF factor is a comprehensive index of thermal performance of HE at constant pumping power.

$$JF = \frac{(j/j_o)}{(f/f_o)^{1/3}} \tag{6}$$

Fig. 10 shows that, JF data of the modified CPHE and the basic CPHE are significantly greater than that of the smooth PHE with the considered Re range. It also shows the heat transfer rate of the modified CPHE is greater than the resistance of the fluid flow (i.e. JF>1). Thus, JF data of the modified CPHE yields the highest values. They are up to 1.4 and 64 times greater than JF data of the basic CPHE and the smooth PHE, respectively.

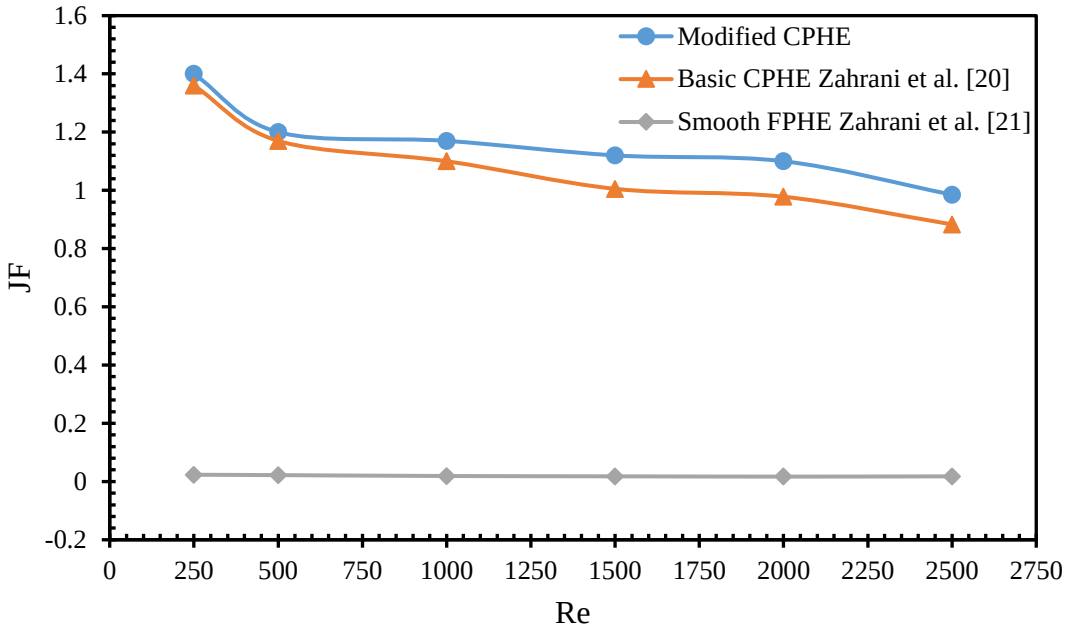

Fig. 10: the overall performance index versus all investgated PHEs.

Turbulence kinetic energy is an indicator of flow mixing and vortex generation. Fig. 11 shows TKE contours for all investigated HEs in the present study inside the same hot channel at Re=2500. It is pronounced that the TKE of the smooth PHE is very low due to the smoothness of its surface. An important observation is that, the TKE at the middle of the channel of the basic CPHE is almost zero which refers to the weakness of the fluid flow in this area. Therefore, the present modification exploits this area to simultaneously promote the flow mixing and enhance the mechanical strength of the HE as each gasket in this area is fully in contact with the previous thermal plate. The TKE attain the maximum values at the corrugation's ridge in both modified and the basic CPHEs. In general, at the same flow rate the intensity of velocity (TKE) of the modified CPHE is about 3.5 times greater than that of the well-known CPHE.

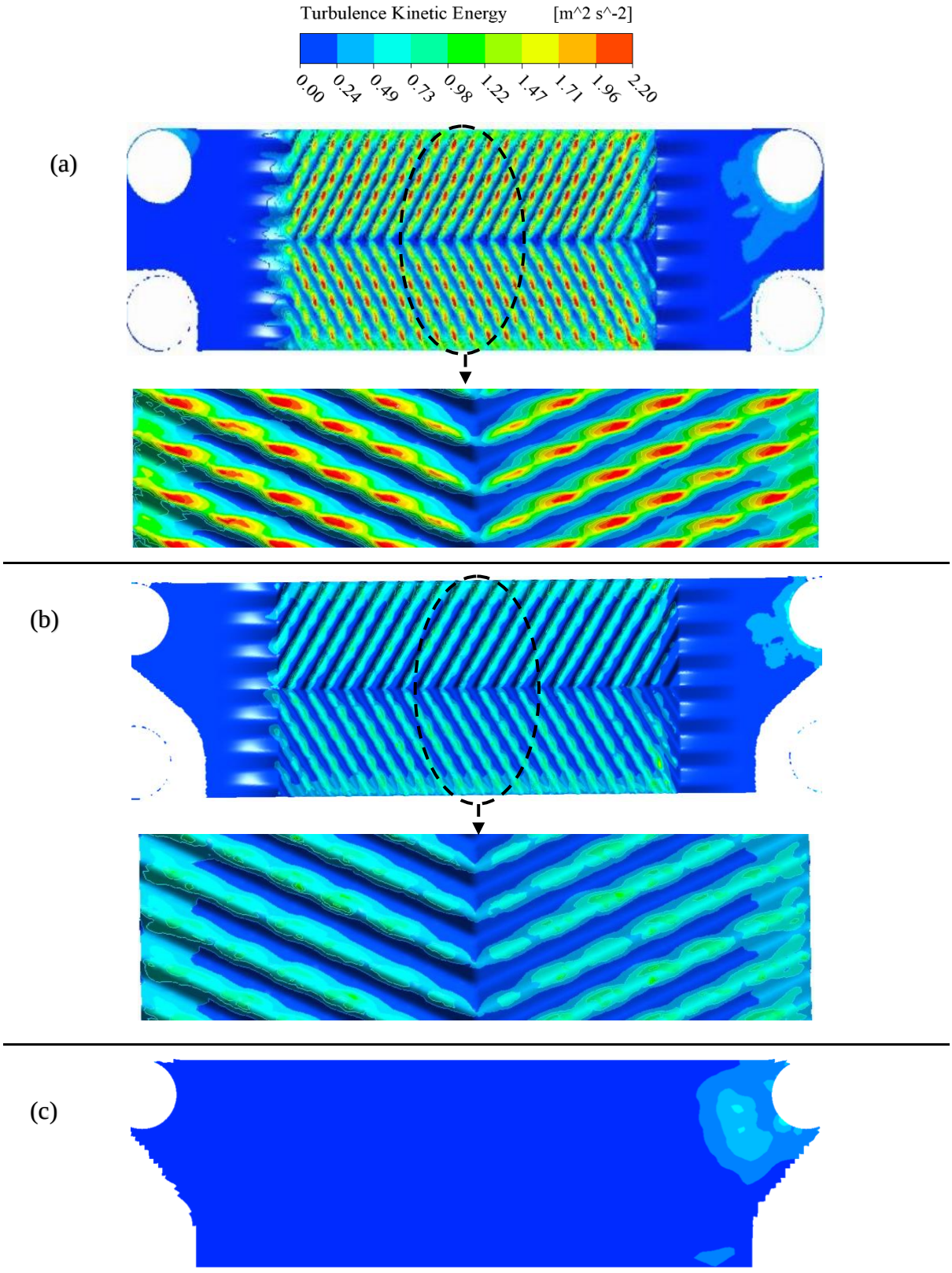

Fig. 11: TKE contours inside the middle hot channel for (a) modified CPHE "enlarge cut part is vertical", (b) basic CPHE "enlarge cut part is vertical", and (c) smooth PHE.

Moreover, the variation in TKE with different Re inside the modified and the basic hot channel are presented in Fig. 12. It shows that, the TKE of the modified channel is 3.3 to 4 times higher

than that of the basic channel which is similar to the TKE data shown in Fig. 11. An important point is this, Fig. 12 shows the maximum enhancement in TKE of the modified channel is taking place at Re=1500. It is ~ 2.4 times higher than TKE data at Re=1000 which is consistent with the data provided in Fig. 8. Therefore, this Re (i.e. Re=1500 to 1600) is the optimum one.

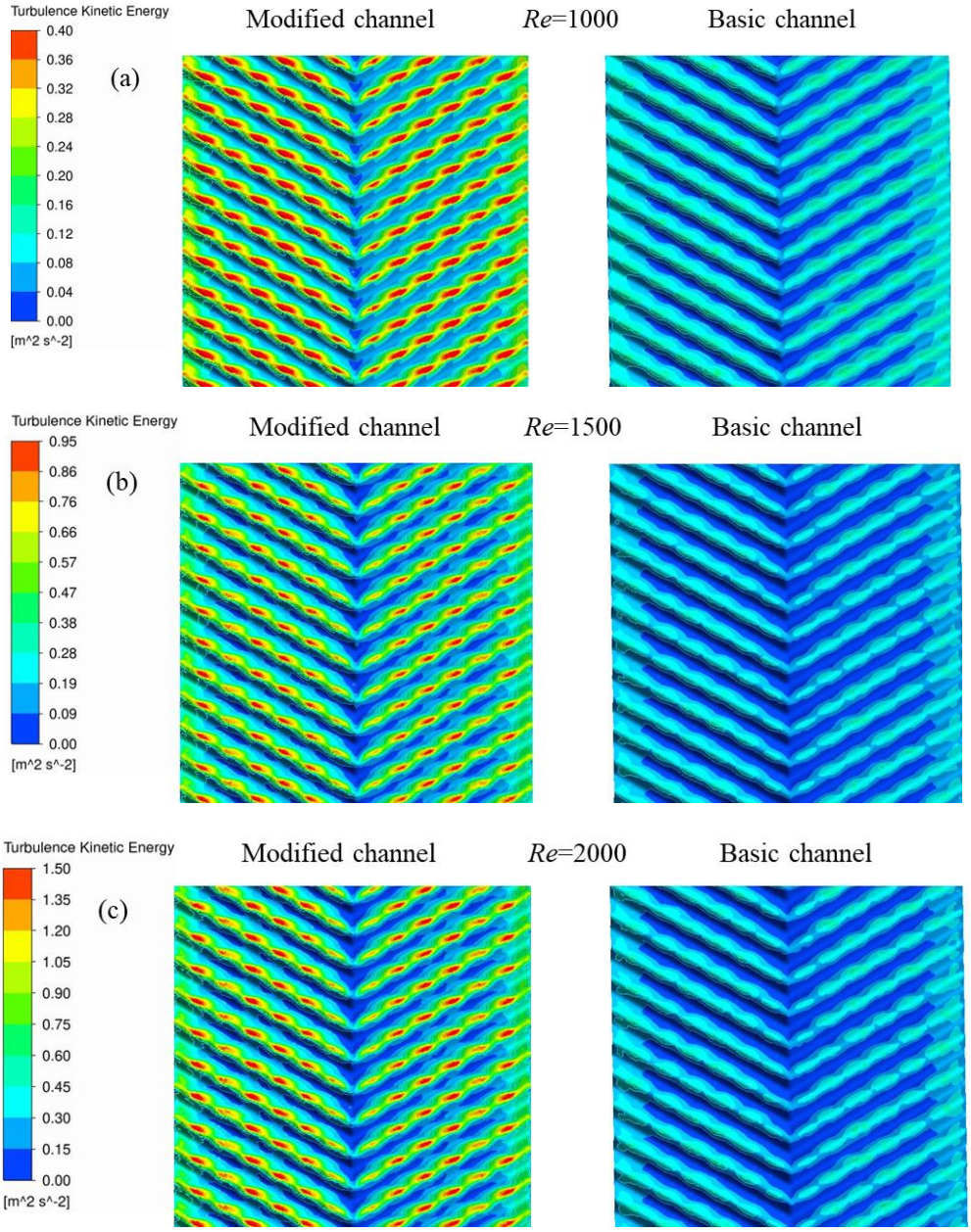

Fig. 12: TKE variation insdie the modified and the basic hot channel at (a) Re=1000, (b) Re=1500, and (c) Re=2000.

Furthermore, in Fig. 13 the velocity vectors at the same location and same mass flow rate inside the hot channel are shown. The velocity vectors inside the modified channel have the greatest magnitude which is consistent with the TKE data in Fig. 11 and 12. Therefore, it is clear that the turbulence rate of the flow has a direct proportionality on the overall thermo-hydraulic performance of the HE which is also confirmed widely in the literature [42].

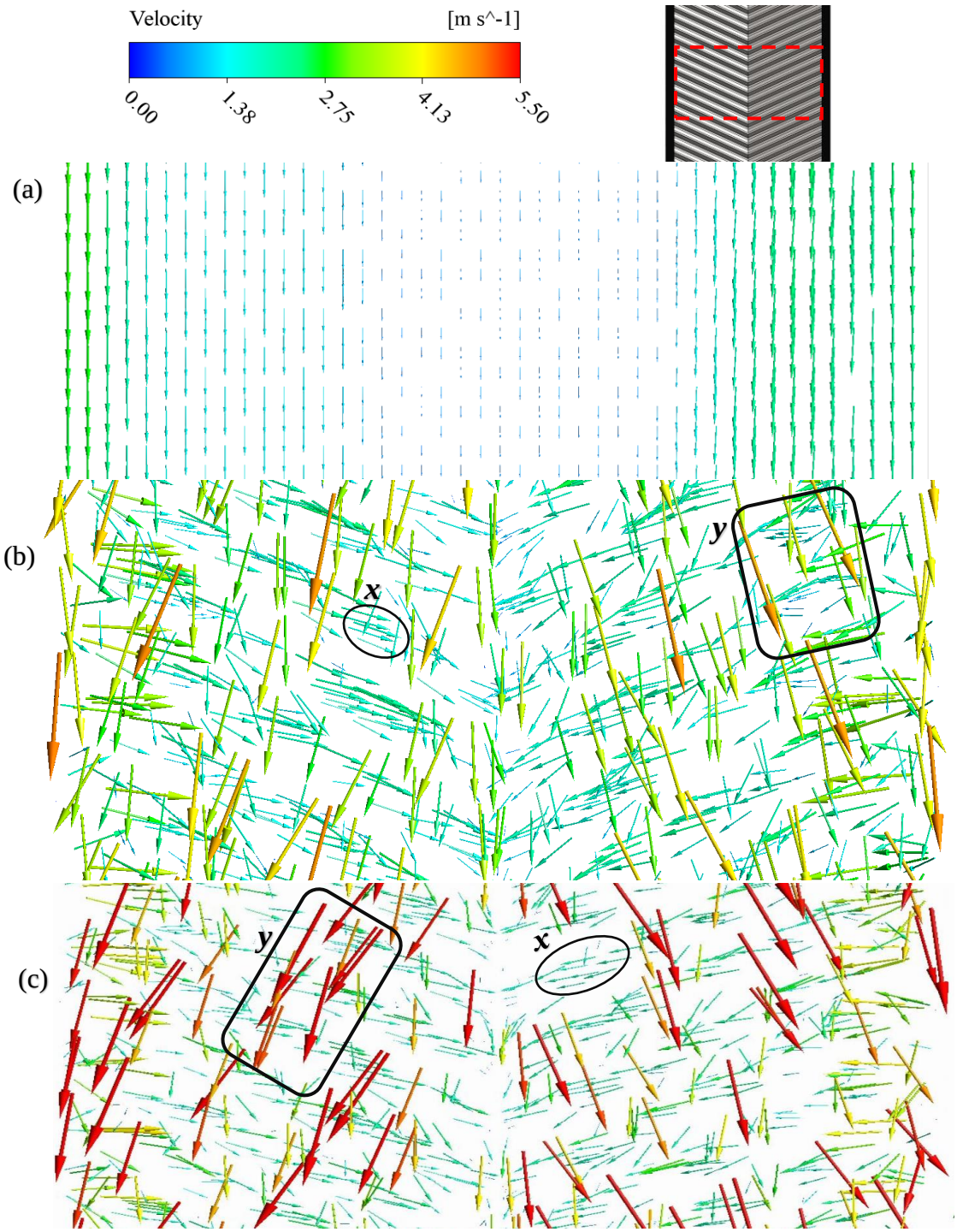

Fig. 13: Velocity vectors at the middle hot channel for all of the present PHEs.

4.3 Fluid flow distribution

The intensity of the randomness of the fluid distribution (P_{mal}) from port to channel is calculated for all the studied HEs. The higher the P_{mal} is, the more deterioration in the thermal performance of the HE. P_{mal} is calculated based on Bassiouny and Martin [10] correlation. The ports' diameters of the inlet and the outlet are identical, thus P_{mal} is:

$$P_{mal} = \left(\frac{NA_\circ}{A_p}\right)^2 \frac{d_e}{fL_p} \quad (7)$$

where N represents the channels number of the investigated fluid, $A_\circ$ and A_p are the cross-sectional areas of the channel flow and the inlet port, respectively. Fig. 14 shows the variation of P_{mal} with different Re.

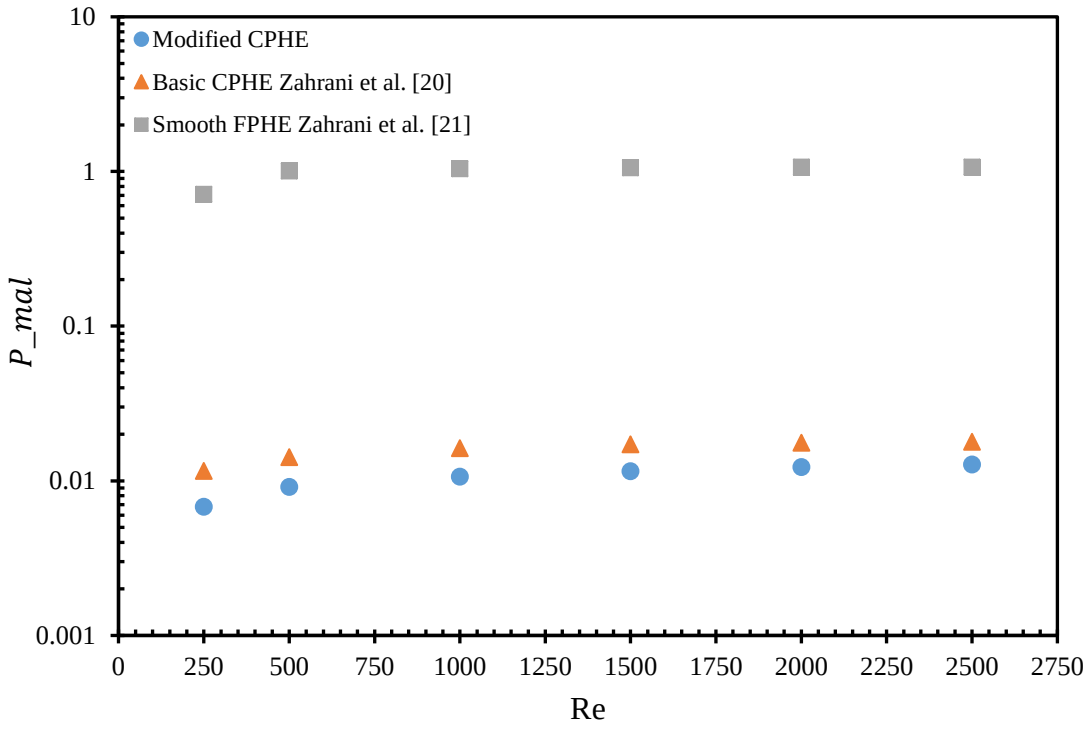

Fig. 14: P_{mal} for all of the present PHEs.

The fluid flow maldistribution of the smooth PHE is the highest. It is up to 70 and 110 times greater than that of the basic and the modified CPHEs, respectively. In addition, for all HEs as Re increases the P_{mal} increases. However, the P_{mal} increasing rate of the modified CPHE is the lowest. The P_{mal} data of all HEs are listed in Table 2.

Table 2: P_{mal} data variation with different Re for all HEs.

Re	P_{mal} FPHE	P_{mal} basic CPHE	P_{mal} modified CPHE
250	0.709006	0.011540637	0.006768
500	1.008267	0.01418115	0.009133
1000	1.039793	0.016230325	0.01063
1500	1.057469	0.017182923	0.011513
2000	1.063817	0.017599768	0.01223
2500	1.067612	0.017873346	0.01275

Additionally, Fig. 13(a) shows that, the fluid with high magnitude tends to flow on the sides of the smooth surface while this magnitude is gradually decreasing till it almost vanishes as the fluid moves toward the middle. Similar flow behavior is observed on the surfaces of the basic and the modified CPHEs. The fluid of the higher magnitude flows transversely to the corrugations toward the sides of the plate as highlighted in (*y*) areas on Fig. 13(b) and (c). Furthermore, the fluid of the low magnitude follows the corrugation path as highlighted in (*x*) areas on Fig. 13(b) and (c). A similar flow pattern has been experimentally found by Lozano et al. [8]. In addition, Fig. 11 shows the TKE contours are consistent with the fluid flow magnitude and the flow direction on the plate's surface. Thus, installing the middle gasket could perform multi-purposes. Mainly it could enhance the thermal performance of the CPHE as it has been demonstrated from all aforementioned heat transfer data. Also lower fluid flow maldistribution from port to channel is achieved. In addition, the fluid flow velocity on the left and the right side of the modified plate has higher magnitude than the velocity on the surface of the basic CPHE as shown in Fig. 13(c). Therefore, this could promote the flow mixing, turbulence intensity, and expedite disruption and re-attachment of the thermal boundary layers resulting in a better heat exchanging process. Another important aspect is that, each middle gasket will be in contact with the previous plate which would increase the mechanical strength of the heat exchanger. Thus, larger range of the maximum operating pressure and temperature could be fulfilled.

4.4 Heat transfer correlations

Nusselt number correlation has been developed based on Sieder empirical correlation [43], as follows:

$$Nu = C_1 Re^p Pr^n \left(\frac{\mu}{\mu_w}\right)^{0.14} \quad (8)$$

Where C_1 represents the constant of the straight line, and p represents the slope of the line. Additionally, the fanning friction factor correlation has been developed based on Kumar empirical correlation [44]:

$$\boldsymbol{f = C_2 Re^m} \quad (9)$$

Nusselt number and fanning friction factor correlations for the basic CPHE and the smooth PHE have been reported in Zahrani et al. [20, 21]. By applying regression technique on the numerical data of the present modified CPHE, Nu and *f* are found as follows:

For $250 \leq Re \leq 2500$

$$Nu = 0.26\, Re^{0.6573} Pr^{1/3} \left(\frac{\mu}{\mu_w}\right)^{0.14} \quad (10)$$

$$f = 8.09\, Re^{-0.2638} \quad (11)$$

The maximum difference between the numerical data of Nu and *f* and the provided correlations are respectively +4% and +5%.

5. Conclusions

Most studies that are performed on PHEs in the literature have investigated the thermal performance of the basic PHEs. However, the current study has presented a newly modified CPHE. The thermal performance of the modified CPHE has been numerically investigated by using CFD approach. To evaluate the impact of the new modification, the result has been compared with the previously reported results of the basic corrugated and smooth PHEs. The geometrical dimensions, physical properties, and boundary conditions are identical for all three HEs. All calculations are performed to the hot side as the process fluid. The essential remarks of this study can be drawn as follows:

- Nusselt number data of the newly modified CPHE is the highest of those for all three HEs. The enhancement in the convective heat transfer is up to 1.3 and 4 times greater than that of the basic corrugated and the smooth PHEs, respectively.
- The increase in the fanning friction factor data of the modified CPHE is up to 1.7 times greater than that of the basic one.
- The TKE attains the maximum values at the corrugation's ridge in both modified and basic CPHEs. The velocity vectors have revealed consistent behavior with the TKE data. The intensity of the TKE inside the modified channel is ~ 3.5 times the TKE inside the basic channel. Thus, TKE is strongly related to the thermo-hydraulic performance of the HE.
- Maximum enhancement in TKE and convective heat transfer of the modified CPHE is taking place at Re~1600.
- In both modified and basic channel, the fluid of the higher magnitude flows transversely with respect to the corrugations toward the sides of the plate whereas the fluid of the low magnitude follows the corrugation path.
- The P_{mal} values are significantly reduced in the modified CPHE where they yield the lowest values. In addition, for all HEs as Re increases the P_{mal} increases. However, the P_{mal} increasing rate of the modified CPHE is the lowest of all three HEs.
- JF data of the modified CPHE yields the highest values, which are up to 1.4 and 64 times greater than JF data of the basic corrugated and the smooth PHEs, respectively.

Generally, the present modification could simultaneously boost the thermal performance and the maximum allowable operating pressure and temperature due to the presence of contact areas at the middle between the plates. In addition, the present modification could be applied for any type of PHE e.g., welded PHE and for any flow arrangement. Thus, it could open up new application areas that require high heat transfer efficiency and could handle high-pressure drop. Finally, further studies are recommended to disclose the additional enhancement in the overall thermal performance of the current modified CPHE when different types of nanofluids are added to the base fluid, and also when different chevron angles (i.e. 30°/30°, and 60°/30°) are used.

Acknowledgement:

Numerical simulations have been executed in the high-performance computing Unit ARCLab, University of Technology Sydney, Australia.

Conflicts of Interest:

The authors declare no conflicts of interest.

References

[1] Agency, I.E., *World energy outlook 2014 executive summary*. 2014.

[2] Syed, A., *The use of plate heat exchangers as evaporators and condensers in process refrigeration.* Heat Exchange Engineering, 1992.

[3] Ayub, Z.H., *Plate heat exchanger literature survey and new heat transfer and pressure drop correlations for refrigerant evaporators.* Heat Transfer Engineering, 2003. 24(5): p. 3-16.

[4] Sundén, B. and R.M. Manglik, *Plate heat exchangers: design, applications and performance*. Vol. 11. 2007: Wit Press.

[5] Li, Q., G. Flamant, X. Yuan, P. Neveu, and L. Luo, *Compact heat exchangers: A review and future applications for a new generation of high temperature solar receivers.* Renewable and Sustainable Energy Reviews, 2011. 15(9): p. 4855-75.

[6] Focke, W. and P. Knibbe, *Flow visualization in parallel-plate ducts with corrugated walls.* Journal of Fluid Mechanics, 1986. 165: p. 73-77.

[7] Tokgoz, N. and B. Sahin, *Experimental studies of flow characteristics in corrugated ducts.* International Communications in Heat and Mass Transfer, 2019. 104: p. 41-50.

[8] Lozano, A., F. Barreras, N. Fueyo, and S. Santodomingo, *The flow in an oil/water plate heat exchanger for the automotive industry.* Applied Thermal Engineering, 2008. 28(10): p. 1109-17.

[9] Tsai, Y.-C., F.-B. Liu, and P.-T. Shen, *Investigations of the pressure drop and flow distribution in a chevron-type plate heat exchanger.* International communications in heat and mass transfer, 2009. 36(6): p. 574-78.

[10] Bassiouny, M. and H. Martin, *Flow distribution and pressure drop in plate heat exchangers—I U-type arrangement.* Chemical Engineering Science, 1984. 39(4): p. 693-700.

[11] Rao, B.P. and S.K. Das, *An experimental study on the influence of flow maldistribution on the pressure drop across a plate heat exchanger.* Journal of Fluids Engineering, 2004. 126(4): p. 680-91.

[12] Durmuş, A., H. Benli, İ. Kurtbaş, and H. Gül, *Investigation of heat transfer and pressure drop in plate heat exchangers having different surface profiles.* International Journal of Heat and Mass Transfer, 2009. 52(5-6): p. 1451-57.

[13] Lin, J., C. Huang, and C. Su, *Dimensional analysis for the heat transfer characteristics in the corrugated channels of plate heat exchangers.* International communications in heat and mass transfer, 2007. 34(3): p. 304-12.

[14] Focke, W., J. Zachariades, and I. Olivier, *The effect of the corrugation inclination angle on the thermohydraulic performance of plate heat exchangers.* International Journal of Heat and Mass Transfer, 1985. 28(8): p. 1469-79.

[15] Mohammed, H., A.M. Abed, and M. Wahid, *The effects of geometrical parameters of a corrugated channel with in out-of-phase arrangement.* International Communications in Heat and Mass Transfer, 2013. 40: p. 47-57.

[16] Nilpueng, K., T. Keawkamrop, H.S. Ahn, and S. Wongwises, *Effect of chevron angle and surface roughness on thermal performance of single-phase water flow inside a plate heat exchanger.* International Communications in Heat and Mass Transfer, 2018. 91: p. 201-09.

[17] Khan, T., M. Khan, M.-C. Chyu, and Z. Ayub, *Experimental investigation of single phase convective heat transfer coefficient in a corrugated plate heat exchanger for multiple plate configurations.* Applied Thermal Engineering, 2010. 30(8-9): p. 1058-65.

[18] Sparrow, E. and L. Hossfeld, *Effect of rounding of protruding edges on heat transfer and pressure drop in a duct.* International Journal of Heat and Mass Transfer, 1984. 27(10): p. 1715-23.

[19] Gürel, B., V.R. Akkaya, M. Göltaş, Ç.N. Şen, O.V. Güler, M.İ. Koşar, and A. Keçebaş, *Investigation on flow and heat transfer of compact brazed plate heat exchanger with lung pattern.* Applied Thermal Engineering, 2020: p. 115309.

[20] Al zahrani, S., M.S. Islam, F. Xu, and S.C. Saha, *Thermal performance investigation in a novel corrugated plate heat exchanger.* International Journal of Heat and Mass Transfer, 2020. 148: p. 119095.

[21] Al zahrani, S., M.S. Islam, and S.C. Sa, *Heat transfer enhancement investigation in a novel flat plate heat exchanger.* International Journal of Thermal Sciences, 2020 (Under review).

[22] Khoshvaght-Aliabadi, M., A. Jafari, O. Sartipzadeh, and M. Salami, *Thermal–hydraulic performance of wavy plate-fin heat exchanger using passive techniques: perforations, winglets, and nanofluids.* International Communications in Heat and Mass Transfer, 2016. 78: p. 231-40.

[23] Khairul, M.A., M.A. Alim, I.M. Mahbubul, R. Saidur, A. Hepbasli, and A. Hossain, *Heat transfer performance and exergy analyses of a corrugated plate heat exchanger using metal oxide nanofluids.* International Communications in Heat and Mass Transfer, 2014. 50: p. 8-14.

[24] Goodarzi, M., A. Amiri, M.S. Goodarzi, M.R. Safaei, A. Karimipour, E.M. Languri, and M. Dahari, *Investigation of heat transfer and pressure drop of a counter flow corrugated plate heat exchanger using MWCNT based nanofluids.* International communications in heat and mass transfer, 2015. 66: p. 172-79.

[25] Bhattad, A., J. Sarkar, and P. Ghosh, *Discrete phase numerical model and experimental study of hybrid nanofluid heat transfer and pressure drop in plate heat exchanger.* International Communications in Heat and Mass Transfer, 2018. 91: p. 262-73.

[26] Sarafraz, M., B. Yang, O. Pourmehran, M. Arjomandi, and R. Ghomashchi, *Fluid and heat transfer characteristics of aqueous graphene nanoplatelet (GNP) nanofluid in a microchannel.* International Communications in Heat and Mass Transfer, 2019. 107: p. 24-33.

[27] Pandey, S.D. and V. Nema, *An experimental investigation of exergy loss reduction in corrugated plate heat exchanger.* Energy, 2011. 36(5): p. 2997-3001.

[28] İpek, O., B. Kılıç, and B. Gürel, *Experimental investigation of exergy loss analysis in newly designed compact heat exchangers.* Energy, 2017. 124: p. 330-35.

[29] Arsenyeva, O., P. Kapustenko, L. Tovazhnyanskyy, and G. Khavin, *The influence of plate corrugations geometry on plate heat exchanger performance in specified process conditions.* Energy, 2013. 57: p. 201-07.

[30] Lee, H., K. Saleh, Y. Hwang, and R. Radermacher, *Optimization of novel heat exchanger design for the application to low temperature lift heat pump.* Energy, 2012. 42(1): p. 204-12.

[31] Zhang, Y., C. Jiang, B. Shou, W. Zhou, Z. Zhang, S. Wang, and B. Bai, *A quantitative energy efficiency evaluation and grading of plate heat exchangers.* Energy, 2018. 142: p. 228-33.

[32] Manglik, R. and J. Ding, *Laminar flow heat transfer to viscous powerlaw fluids in double-sine ducts.* International Journal of Heat and Mass Transfer, 1997. 40(6): p. 1379-90.

[33] Metwally, H. and R.M. Manglik, *Enhanced heat transfer due to curvature-induced lateral vortices in laminar flows in sinusoidal corrugated-plate channels.* International Journal of Heat and Mass Transfer, 2004. 47(10-11): p. 2283-92.

[34] Al zahrani, S., M.S. Islam, and S.C. Saha, *A thermo-hydraulic characteristics investigation in corrugated plate heat exchanger.* Energy Procedia, 2019. 160: p. 597-605.

[35] Dewan, A., P. Mahanta, K.S. Raju, and P.S. Kumar, *Review of passive heat transfer augmentation techniques.* Proceedings of the Institution of Mechanical Engineers, Part A: Journal of Power and Energy, 2004. 218(7): p. 509-27.

[36] Kandlikar, S. and R. Shah, *Multipass plate heat exchangers—effectiveness-NTU results and guidelines for selecting pass arrangements.* Journal of Heat Transfer, 1989. 111(2): p. 300-13.

[37] Rao, B.P. and S.K. Das, *Effect of flow distribution to the channels on the thermal performance of the multipass plate heat exchangers.* Heat Transfer Engineering, 2004. 25(8): p. 48-59.

[38] Ansys, *Ansys fluent 12.0 user's guide.* 2009.

[39] Dorfman, A.S., *Conjugate problems in convective heat transfer*. 2009: CRC Press.

[40] Lee, J. and K.-S. Lee, *Friction and Colburn factor correlations and shape optimization of chevron-type plate heat exchangers.* Applied Thermal Engineering, 2015. 89: p. 62-69.

[41] Kumar, H. *The plate heat exchanger: construction and design*. in *Institute of Chemical Engineering Symposium Series*. 1984.

[42] Wang, Y., F. Houshmand, D. Elcock, and Y. Peles, *Convective heat transfer and mixing enhancement in a microchannel with a pillar.* International Journal of Heat and Mass Transfer, 2013. 62: p. 553-61.

[43] Sieder, E.N. and G.E. Tate, *Heat transfer and pressure drop of liquids in tubes.* Industrial & Engineering Chemistry, 1936. 28(12): p. 1429-35.

[44] Kumar, H. *Evaporation in Plate Heat Exchangers*. in *AICHE Symposium Series*. 1993. American Institute Of Chemical Enginners.